

# Sulfur and Chlorine K-Edge X-ray Absorption Spectroscopic Studies of Photographic Materials

Teresa A. Smith,<sup>\*,†</sup> Jane G. DeWitt,<sup>‡§</sup> Britt Hedman,<sup>\*,||</sup> and Keith O. Hodgson<sup>\*,‡,||</sup>

Contribution from Imaging Research and Advanced Development, Eastman Kodak Company, Rochester, New York 14650, Department of Chemistry, Stanford University, Stanford, California 94305, and Stanford Synchrotron Radiation Laboratory, Stanford University, SLAC, M.S. 69, P.O. Box 4349, Stanford, California 94309

Received November 15, 1993\*

**Abstract:** The sulfur and chlorine centers in sensitizing dyes and surface-modifying agents of importance to the photographic system were characterized by S and Cl K-edge X-ray absorption spectroscopy (XAS). The K-edge spectra of these compounds reveal sharp, characteristic absorption features that provide direct information about the local electronic and geometric environment of the absorber centers. In particular, a sharp, intense pre-edge feature at 2470–2472 eV is observed in the spectra of compounds containing exocyclic S (thione or thiol) that has no counterpart in the spectra of thiazole-containing (cyclic S) compounds. Single-crystal polarized spectra reveal that the edge features of these compounds exhibit a strong orientational dependence, permitting the assignment of some of the observed features. The exocyclic S pre-edge feature was assigned to a S 1s →  $\pi^*$  transition, while the predominant spectral feature at 2473–2474 eV observed in all of the S K-edge spectra was found to be polarized along the C–S bond direction and assigned to a S 1s →  $\sigma^*$  transition. Dramatic changes in the sulfur–ligand spectral features are produced from complexation with Ag and Au atoms, which permits the distinction of covalent *vs* ionic interactions with the metals encountered in photographic systems. Covalent metal interaction with an exocyclic S-containing ligand resulted in the disappearance of the low-energy  $\pi^*$  pre-edge feature, while the intensity of the predominant  $\sigma^*$  feature in all compounds investigated was greatly enhanced upon complexation with Au and Ag metals. In contrast to the uncomplexed ligands, this predominant feature was found to be most intense for polarizations along the S–metal direction and perpendicular to the C–S bond, indicating a direct bonding interaction with the Au metal, as seen, for example, in a bis(ethylenethiourea) Au(I) complex. The K-edge spectra of Cl centers, present as substituents on the ring system of the dye molecules, exhibit a single predominant feature at approximately 2825 eV, which is characteristic of the terminal C–Cl environment and is relatively insensitive to structural changes in the dye systems more remote from the Cl centers. Single-crystal measurements revealed that this spectral feature is polarized predominantly along the C–Cl bond direction, indicating that it is due primarily to a Cl 1s →  $\sigma^*$  transition with some contribution from a lower-intensity transition to a near-lying  $\pi$ -symmetry orbital. The results of these studies form the basis for the interpretation of polarized surface measurements at a glancing angle configuration of a dyed AgBr sheet crystal, which suggest that there is no covalent interaction between the terminal sulfur centers in the merocyanine dye molecules and the silver ions on the AgBr substrate surface. In addition, the polarization properties of the S and Cl K-edge features provide insight into the orientation of the dye molecules on the AgBr substrate, indicating that the dye molecules are adsorbed in an edge-on fashion.

## Introduction

Several crucial elements of the photographic system including sensitizing dyes, surface-modifying agents, and chemical sensitization centers contain sulfur and chlorine atoms incorporated in species on the surface of the photoactive silver halide microcrystals. These centers are involved in surface electron transfer and energy-transfer processes and are, therefore, of critical interest for their importance to the photographic process. The structure of surface species has a pronounced effect on photographic performance. Synchrotron radiation X-ray absorption spectroscopy (XAS) at the sulfur and chlorine K-edges (2–3 keV) can probe these important surface-active molecules and provide a direct measure of the geometric and electronic structure of these molecules on the photoactive substrate. Some of our initial sulfur K-edge results showing the potential of this physical technique for investigating photographic materials were reported previously.<sup>1</sup> The studies reported here expand upon this initial

work to include both sulfur and chlorine K-edge measurements of dyes, silver ligands, and their metal complexes.

Sensitizing dyes are used in many applications such as nonlinear optics, solar energy conversion, electrophotography, and silver halide photography. Merocyanine and cyanine dyes extend the response of photographic materials beyond the intrinsic blue/ultraviolet absorption of the silver halide photoconductor into the visible and infrared regions. The spectral sensitivity imparted to the silver halide substrate depends on the visible absorption properties of the dye molecules. Aggregation of the dye molecules on the surface produces large spectral shifts and significant changes in the absorption band shape. These spectral changes depend on the concentration and orientation of the dye molecules. The extent of aggregation and, consequently, the spectral shift, are in part determined by the silver halide surface composition and morphology, the presence of other adsorbates, and structural features of the dye molecules themselves.<sup>2</sup> Chlorine is a common substituent on many merocyanine and cyanine dye nuclei and can influence the aggregation properties of dye molecules.

The sensitization process involves the transfer of electrons or energy from the photoexcited state of the dye molecule aggregate into the conduction band of the silver halide substrate and requires that the dye molecules exist in an adsorbed state on the surface

<sup>†</sup> Eastman Kodak Co.

<sup>‡</sup> Department of Chemistry, Stanford University.

<sup>§</sup> Present address: Life Sciences Division, Los Alamos National Laboratory, Los Alamos, NM 87545.

<sup>||</sup> Stanford Synchrotron Radiation Laboratory.

\* Abstract published in *Advance ACS Abstracts*, April 1, 1994.

(1) Smith, T. A.; DeWitt, J. G.; Hodgson, K. O.; Hedman, B. In *X-ray Absorption Fine Structure*; Hasnain, S. S., Ed.; Ellis-Horwood: Chichester, England, 1991; pp 607–609 (published Proc. XAFS VI Conf.).

(2) Herz, A. H. *Adv. Colloid Interface Sci.* 1977, 8, 237–298.

of the silver halide grains. The nature of the interaction between the dye aggregates and the silver halide substrate has been the subject of many studies. For dyes containing sulfur groups, it has been postulated that the adsorbed dye molecules are oriented with their sulfur atoms directed toward the silver halide surface.<sup>3,4</sup> X-ray photoelectron spectroscopic (XPS) experiments of dyed AgCl crystals<sup>5</sup> and electrophoretic mobility studies of dyed silver halide grains<sup>6</sup> have suggested that direct interaction between the sulfur atoms and the silver ions on the crystal surface is a driving force in the adsorption process and a determining factor in the orientation of dye molecules on silver halide crystal faces.

Other sulfur-containing silver ligands such as mercaptotetrazoles, thioureas, and thiazoline thiones used as additives in photographic materials can be adsorbed to the silver halide surface and may act as antifoggants, crystal growth accelerators, or development inhibitors. Previous XPS studies<sup>7,8</sup> have indicated that some compounds of these types are adsorbed to the silver halide surface via coordination between the ligand sulfur atoms and the surface silver ions.

Previous sulfur XAS studies have shown that the S and Cl K-edge spectra are characterized by sharp absorption features in the edge and near-edge region arising from bound-state transitions from the 1s orbital to low-lying, unoccupied, or partially occupied atomic or molecular orbitals. Studies of the sulfur K-edge spectra of numerous organic and inorganic compounds have revealed characteristic absorption features dependent on the local geometry and oxidation state of the absorbing sulfur atom.<sup>9-11</sup> With a spectrometer energy resolution of  $\sim 0.5$  eV at these energies (2–3 keV), shifts of as much as 13 eV have been seen with a change in the oxidation state of sulfur from  $-2$  to  $+6$ . A number of soft X-ray studies have been done on gaseous<sup>12</sup> and surface-adsorbed<sup>12a,13</sup> organic and inorganic sulfur-containing molecules, such as thiols, thioethers, and sulfuryl halides. These studies provide insight into the origin and nature of the K-edge features, including information about the symmetry of the final-state orbitals to which the transition occurs, and the orientation dependence of the edge features of adsorbed species.<sup>12a,b,14</sup> Polarized K-edge measurements together with theoretical calculations using a multiple scattered wave  $X\alpha$  formalism have resulted in assignments of some of the K-edge features of sulfur- and chlorine-containing oxyanions.<sup>15</sup>

We have used S and Cl K-edge XAS to investigate the electronic and geometric structure of a wide variety of surface compounds important to the photographic system, including cyanine and merocyanine dye nuclei and other sulfur-containing silver ligands

such as thioureas, mercaptotetrazoles, and other thione/thiolate compounds. The nature of the interaction between the surface metal ions and the forms of sulfur of importance in the photographic system have been probed by the measurement of S K-edge XAS of silver and gold complexes of these sulfur ligands. The highly polarized nature of synchrotron radiation permits the determination of the angular dependence of the K-edge features by the measurement of oriented single-crystal polarized spectra of representative dye nuclei and metal-sulfur compounds. From these studies, we are able to make assignments to some of the X-ray absorption features that provide the basis for the interpretation of polarized surface measurements at grazing incidence of dye molecules on silver bromide sheet crystals.

## Experimental Section

**Chemical Samples.** Molecular structures and abbreviated sample names of the chemicals discussed in this paper are presented in Tables 1–3. Many additional samples not directly addressed in this paper for which X-ray absorption data were collected are found in supplementary tables, S-I, S-II, and S-III. With the exception of the thiazoline thione (CMMTT) and triazolium thiolate (TRZ) compounds, all sulfur ligands (Table 2) and the  $\beta$ -9,10-dichloroanthracene sample (Table 1) were purchased from various chemical suppliers (Aldrich, Alfa, etc.). The silver and gold complexes (Table 3) and the CMMTT and TRZ ligands, as well as all of the dye samples (Table 1), were synthesized in the research laboratories of Eastman Kodak Co.

Single-crystal samples were grown according to the procedures in the published literature. Crystals of 2-thiohydantoin<sup>16</sup> (M4) were obtained from ethanol as orange rhombic plates with sides 1–2 mm long and 0.3–0.5 mm thick. Yellow needles of 3,3'-diethylthiacyanine bromide<sup>17</sup> (C4) were obtained from propanol (1–2 mm  $\times$   $\sim 0.25$  mm  $\times$   $\sim 0.25$  mm). Single crystals of  $\beta$ -9,10-dichloroanthracene<sup>18</sup> (DCA) were obtained from saturated petroleum ether solutions of the compound placed in a desiccator containing scraps of paraffin. The crystals were yellow plates of dimensions 1–2 mm  $\times$  0.3 mm  $\times$   $< 0.3$  mm. White single crystals of bis(ethylenethiourea) gold(I) chloride hydrate<sup>19</sup> were obtained from water. The crystals were parallelepipeds, 2 mm  $\times$  1 mm  $\times$  0.5 mm. The integrity of the crystals after exposure to synchrotron radiation was verified by checking that degradation of the diffraction quality of the crystal had not occurred and by confirming the unit cell dimensions using a four-circle diffractometer after the conclusion of the experiments.

AgBr sheet crystals (50  $\mu$ m thick) were grown on quartz plates using a growth gradient technique.<sup>20</sup> The dyed surface sample was prepared by submerging the sheet crystal in  $10^{-5}$  M aqueous solutions of the dye for 20 min at 40 °C with stirring.

**X-ray Absorption Measurements.** Experiments were conducted on the unfocused 8-pole wiggler beamline 4-1 and the focused 54-pole wiggler beamline 6-2 (in low magnetic field mode)<sup>9</sup> at Stanford Synchrotron Radiation Laboratory (3.0 GeV, 40–80 mA) and on unfocused bending magnet beamlines X19A and X10C at the National Synchrotron Light Source (2.5 GeV, 90–200 mA) by using Si (111) double-crystal monochromators. Higher harmonics were rejected by detuning the monochromator 80% at 2740 eV for the sulfur edge and 60% at 3250 eV for the chlorine edge on beamline 4-1. On beamline 6-2, higher harmonics were minimized using a procedure in which layers of Al foil were placed between the sample holder and the detector and the monochromator was detuned at 2740 eV for S and 3150 eV for Cl until the fluorescent signal approached dark current level, resulting in  $\sim 20\%$  detuning. Incident radiation was detuned 20–30% at 2740 eV on beamlines X19A and X10C. Beam size for the powder samples was defined by Ta slits to be 2  $\times$   $\sim 15$  mm except on beamline 6-2, on which it was defined by the focusing mirror to be  $\sim 1.5 \times 4.0$  mm. For the single-crystal samples, the incident beam size was defined by Ta slits to be slightly larger than the size of the crystal in the appropriate orientation. For the polarized surface measurements (performed on beamline 6-2 at SSRL), the width of the beam was determined by the size of the focusing optics. Slits were set to allow the maximum amount of sample to be illuminated by a narrow

(3) Bird, G. R.; Norland, K. S.; Rosenoff, A. E.; Michaud, H. B. *Photogr. Sci. Eng.* **1968**, *12*, 196–206.

(4) Ficken, G. E. *J. Photogr. Sci.* **1973**, *21*, 11–18.

(5) Saijo, H.; Kitamura, T.; Ohtani, H. *Surf. Sci.* **1986**, *177*, 431–443.

(6) Weiss, G.; Ericson, R.; Herz, A. *J. Colloid Interface Sci.* **1967**, *23*, 277–285.

(7) Tani, T. *J. Imaging Sci.* **1988**, *32*, 227–231.

(8) Tani, T. *Photogr. Sci. Eng.* **1977**, *21*, 317–325.

(9) Hedman, B.; Frank, P.; Penner-Hahn, J. E.; Roe, A. L.; Hodgson, K. O.; Carlson, R. M. K.; Brown, G.; Cerino, J.; Hettel, R.; Troxel, T.; Winick, H.; Yang, J. *Nucl. Instrum. Methods* **1986**, *A246*, 797–800.

(10) Lytle, F. W.; Greeger, R. B.; Sandstrom, D. R.; Marques, E. C.; Wong, J.; Spiro, C. L.; Huffman, G. P.; Huggins, F. E. *Nucl. Instrum. Methods* **1984**, *226*, 542–548.

(11) (a) Sugiura, C. *J. Chem. Phys.* **1983**, *79*, 4811–4814. (b) George, G. N.; Gorbaty, M. L. *J. Am. Chem. Soc.* **1989**, *111*, 3182–3186.

(12) (a) Hitchcock, A. P.; Horsley, J. A.; Stöhr, J. *J. Chem. Phys.* **1986**, *85*, 4835–4848. (b) Dezarnaud, C.; Tronc, M.; Hitchcock, A. P. *J. Chem. Phys.* **1990**, *142*, 455–462. (c) Perera, R. C. C.; LaVilla, R. E. *J. Chem. Phys.* **1984**, *81*, 3375–3382. (d) Hitchcock, A. P.; Bodeur, S.; Tronc, M. *J. Chem. Phys.* **1987**, *115*, 93–101. (e) Hitchcock, A. P.; Tronc, M. *J. Chem. Phys.* **1988**, *121*, 265–277. (f) Sze, K. H.; Brion, C. E.; Tronc, M.; Bodeur, S.; Hitchcock, A. P. *J. Chem. Phys.* **1988**, *121*, 279–297.

(13) (a) Yakata, Y.; Yoiyama, T.; Yagi, S.; Hapoo, N.; Sato, H.; Seki, K.; Ohta, T.; Kitajima, Y.; Kuroda, H. *Surf. Sci.* **1991**, *259*, 266–274. (b) Seymour, D. L.; Bao, S.; McConville, C. F.; Crapper, M. D.; Woodruff, D. P.; Jones, R. G. *Surf. Sci.* **1987**, *189/190*, 529–534. (c) Stöhr, J.; Kollin, E. B.; Fischer, D. A.; Hastings, J. B.; Zaera, F. *J. Phys. Rev. Lett.* **1985**, *55*, 1468–1471.

(14) Stöhr, J.; Outka, D. A. *J. Phys. Rev. B* **1987**, *36*, 7891–7905.

(15) Tyson, T. A.; Roe, A. L.; Hodgson, K. O.; Hedman, B. *J. Phys. Rev. B* **1989**, *39*, 6305–6315.

(16) Walker, L. A.; Folting, K.; Merritt, L. L., Jr. *Acta Crystallogr.* **1969**, *B25*, 88–93.

(17) Nakatsu, K.; Yoshioka, H.; Aoki, T. *Chem. Lett.* **1972**, 339–340.

(18) Trotter, J. *Acta Crystallogr.* **1986**, *C42*, 862–864.

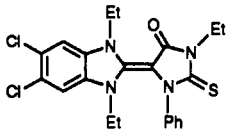
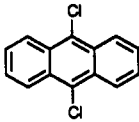
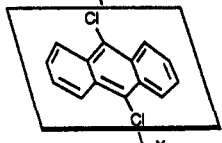
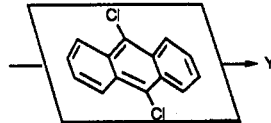
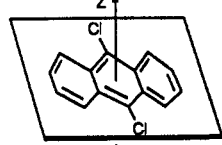
(19) Jones, P. G.; Guy, J. J.; Sheldrick, G. M. *Acta Crystallogr.* **1976**, *B32*, 3321–3322.

(20) Clark, P. V. McD.; Mitchell, J. W. *J. Photogr. Sci.* **1956**, *4*, 1–20.

**Table 1.** Energies of Transitions in the S and Cl K-Edge Spectra of Dyes and Dye Intermediates

sample name	structure	S K-edge			Cl K-edge	
		feature A' (eV)	feature A (eV)	feature B (eV)	feature A (eV)	feature B (eV)
<b>Cyanine Dyes and Dye Nuclei</b>						
C1			2473.5 <sup>a</sup>	2475.3		
C2			2473.8 <sup>a</sup>	2475.8	2825.0 <sup>a</sup>	2830.6
C3			2474.0 <sup>a</sup>	2476.2		
C4 (powder)			2473.8 <sup>a</sup>	2475.6 2476.4 (sh)		
C4X (single-crystal) in-plane orientation			2473.5 <sup>a</sup>	2475.1		
C4Z (single-crystal) out-of-plane orientation			2473.9 <sup>a</sup>	2475.6 (sh) 2476.5		
<b>Merocyanine Dyes and Dye Intermediates</b>						
M1		2470.5 2471.9 (sh)	2473.6 <sup>a</sup>	2478.2	2825.0 <sup>a</sup>	2831.0
M2		2471.4	2473.7 <sup>a</sup>	2477.3		
M3		2470.9 2472.4 (sh)	2474.0 <sup>a</sup>	2476.6	2825.1 <sup>a</sup>	
M4 (powder)		2471.4	2473.8 <sup>a</sup>	2477.5		
M4X (single-crystal) X orientation in-plane, along C=S		2471.3 (sh)	2473.8 <sup>a</sup>	2475.9 (sh) 2477.8		
M4Y (single-crystal) Y orientation in-plane, perp to C=S		2471.2 (sh)	2473.7 <sup>a</sup>	2476.5		
M4Z (single-crystal) Z orientation out-of-plane		2471.3 <sup>a</sup>	2473.4 (sh)	2477.4		

Table 1 (Continued)

sample name	structure	S K-edge			Cl K-edge	
		feature A' (eV)	feature A (eV)	feature B (eV)	feature A (eV)	feature B (eV)
M5		2471.2	2473.4 <sup>a</sup>	2477.0	2824.8 <sup>a</sup>	2828.2 2831.4
<b>Polarized Single Crystal at Cl K-Edge</b>						
DCA (powder) dichloroanthracene					2825.0 <sup>a</sup>	2830.5
DCAX (single crystal) X orientation, in-plane, parallel to Cl-Cl					2825.0 <sup>a</sup>	2827.9 2831.3
DCAY (single-crystal) Y orientation, in-plane, perp to Cl-Cl					2825.0 <sup>a</sup>	2827.9 2829.4 2831.7
DCAZ (single-crystal) Z orientation, out-of-plane					2824.6 <sup>a</sup>	2827.2 2830.4

<sup>a</sup> Most intense feature.

band of beam ( $7 \times 1$  mm for  $\chi = 0^\circ$ ,  $5 \times 2$  mm for  $\chi = 90^\circ$ ). The entire experimental hutch was kept under red safelight conditions for the measurement of photosensitive samples.

Data were collected at room temperature in fluorescence mode using a  $N_2$ -filled gas ionization detector of the Stern/Heald/Lytle design.<sup>10,21</sup> Powder samples were finely ground in a mortar and dusted onto Mylar tape to avoid self-absorption effects. At the low energies at which these experiments were conducted ( $\sim 2460$  to  $\sim 3200$  eV), reduction in incident radiation intensity by air absorption is of major concern. To alleviate this problem, the experiment was conducted under a helium beam path for the incident radiation and sample fluorescence. Polypropylene windows of 6.3- $\mu$ m thickness were used where necessary. Scans of  $Na_2S_2O_3 \cdot 2H_2O$  and  $CsCuCl_4$  collected between sample measurements were used to calibrate the energy of the sample spectra by assigning the position of the first peak in the scans to 2472.02 and 2820.30 eV, respectively. For each sample, two to five calibrated scans were averaged and the inherent background in the data was removed by fitting a polynomial to the preedge region, which was extrapolated through the entire spectrum and subtracted. The data were normalized to an edge jump of unity for direct comparisons of intensities of features. The energy positions of the edge features listed in Tables 1–3 were determined by locating the position of the half-width at half-maximum of the second derivative in the region of the feature of interest.

**Oriented Single-Crystal Polarized Measurements.** For electronic dipole-coupled transitions, the features seen in the K-edge spectra are governed by the following relation:

$$\sigma = |\langle \Psi_f | e \cdot r | \Psi_i \rangle|^2 \quad (1)$$

which can be approximated by

$$\sigma = \cos^2 \theta |\langle \Psi_f | r | \Psi_i \rangle|^2 \quad (2)$$

where  $\sigma$  is the photoabsorption cross section,  $\Psi_f$  is the final state wave function,  $\Psi_i$  is the initial state wave function (S or Cl 1s orbital for the

cases herein),  $e$  is the polarization vector of the incident radiation (perpendicular to the direction of the incident radiation and in the plane of the synchrotron ring),  $r$  is the transition dipole operator ( $x$ ,  $y$ , or  $z$ ), and  $\theta$  is the angle between  $e$  and  $r$ . For K-edges, the dipole-allowed transitions from the totally symmetric initial 1s state are to final p states ( $\Delta l = \pm 1$ ), which transform as the dipole operators  $x$ ,  $y$ , or  $z$ . The maximum in the photoabsorption cross section is obtained when  $\theta = 0^\circ$ , when the polarization vector and the dipole operator are parallel. For powder or solution samples, the average isotropic spectrum will contain a superposition of the polarized spectral features of all three molecular dipoles ( $x$ ,  $y$ ,  $z$ ) averaged over all possible orientations ( $\theta$ ). In the polarized single-crystal spectra these superimposed features may be resolved and assigned to their appropriate final-state symmetries ( $p_x$ ,  $p_y$ , or  $p_z$ ) by determining the angular dependence of the transition intensities as a function of molecular alignment. By aligning a molecular vector in the sample (for example, a C–S bond) with the direction of the incident radiation polarization vector, one can selectively excite transitions into the orbitals along that molecular orientation.

The single crystals used in this study have been structurally characterized by X-ray diffraction.<sup>16–19</sup> X-ray diffraction measurements on the obtained single-crystal samples were compared with published values of cell parameters and found to be consistent. The published atomic coordinates were used to determine the orientation of specific molecular directions with respect to the crystal axes and thus the ( $hkl$ ) indices of crystal lattice planes perpendicular to these molecular directions.

The samples were preoriented on a Siemens P3 four-circle diffractometer by determining the  $\varphi$  angle settings (at  $\chi = 0^\circ$ ) required to bring these lattice planes into a diffraction position. Single crystals were mounted on glass fibers using a standard 5-min epoxy (that contains S) for the Cl-containing crystals and polymethyl methacrylate in methylene chloride as the adhesive for the S-containing crystals and were attached on a standard goniometer head. The crystals were mounted in such a fashion that only  $\varphi$  angle rotations were required to attain the desired crystal orientations. This geometric restriction meant that more than one crystal was required to isolate all of the orientations of interest. The diffractometer geometry is such that, at the determined  $\varphi$  and  $\chi$  settings, the molecular vector will be perpendicular to both the direction of the

**Table 2.** Energies of Transitions in S K-Edge Spectra of Thione- and Thiol-Containing Ligands

compound	structure	sample name	feature A' (eV)	feature A (eV)	feature B (eV)
3-(carboxymethyl)-4-methyl-4-thiazoline-2-thione		CMMTT	2471.3	2474.3 <sup>a</sup>	2476.2
thiourea		THIOUR	2472.0	2473.2	2475.7 (sh) 2477.5 <sup>a</sup>
tetramethylthiourea		TMTU	2471.4	2473.2	2474.7 (sh) 2476.0 <sup>a</sup>
ethylenethiourea		ETU	2472.0	2473.4	2475.1 (sh) 2476.7 <sup>a</sup>
2-ethylmercaptotetrazole		EMT	2472.5 (wk sh)	2473.2 <sup>a</sup>	2476.2
2-phenylmercaptotetrazole		PMT	2471.8	2473.6 <sup>a</sup>	2476.3 (sh) 2478.2
2-(acetamidophenyl)mercaptotetrazole		APMT	2471.8	2473.5 <sup>a</sup>	2475.9 (sh) 2477.7
2-(acetamidophenyl)mercaptotetrazole sodium salt		APMTNA	2472.2 (wk sh)	2473.2 <sup>a</sup>	2476.7
1,4,5-trimethyl-1,2,4-triazolium-3-thiolate		TRZ	2472.4 (sh)	2473.2 <sup>a</sup>	2474.9

<sup>a</sup> Most intense feature.**Table 3.** Energies of Transitions in Silver- and Gold-Sulfur Complexes

compound	sample name	feature A (eV)	feature B (eV)
silver(I) 3-(carboxymethyl)-4-methyl-4-thiazoline-2-thione hydrate tetrafluoroborate	AGCMMTT	2473.7 2471.8 (sh)	2476.1
silver(I) phenylmercaptotetrazole	AGPMT	2473.3 <sup>a</sup>	
silver(I) bis(trimethyltriazolium thiolate) tetrafluoroborate, polymer	AGTRZ2	2473.3 <sup>a</sup>	
gold(I) thiourea tetrafluoroborate	AUTHIOUR	2473.3 <sup>a</sup>	2475.0
gold(I) tetramethylthiourea tetrafluoroborate	AUTMTU	2473.3 <sup>a</sup>	2474.9
gold(I) bis(trimethyltriazolium thiolate) tetrafluoroborate	AUTRZ2	2472.6 (sh) 2473.5 <sup>a</sup>	2475.1
gold(I) bis(ethylenethiourea) chloride hydrate (powder)	AUETU2	2473.3 <sup>a</sup>	2475.3
gold(I) bis(ethylenethiourea) chloride hydrate (single crystal) in-plane polarized, along C-S	AUETU2X	2473.9	2475.3 <sup>a</sup>
gold(I) bis(ethylenethiourea) chloride hydrate (single crystal) in-plane polarized, along Au-S	AUETU2Y	2473.4 <sup>a</sup>	2475.4
gold(I) bis(ethylenethiourea) chloride hydrate (single crystal) out-of-plane polarized	AUETU2Z	2473.2 <sup>a</sup>	2474.5 2475.6

<sup>a</sup> Most intense feature.

incident radiation beam and the goniometer head axis. On the beamline, a lid to the sample chamber containing a goniometer mount was used, allowing full rotation in  $\varphi$  with  $\chi$  fixed at  $180^\circ$ . By duplicating this diffractometer geometry in the sample chamber on the beamline, the molecular vectors were aligned parallel to the electric field vector ( $\mathbf{e}$ ) of the polarized incident radiation beam.

Polarized spectra were measured at crystal orientations that maximized the projections of individual symmetry-related molecular vectors on the direction of polarization. These orientations were determined from the average of symmetry-related molecular vectors according to the crystal space group. The 2-thiohydantoin (M4) and  $\beta$ -9,10-dichloroanthracene (DCA) crystals belong to monoclinic space groups with noninversion-symmetry-related individual molecular vectors related by reflection through the  $ac$  crystal plane. For these compounds the three orientations that maximize the individual molecular  $x$ ,  $y$ , and  $z$  polarizations are achieved with alignments along the crystal  $b$  axis and two  $ac$  projections of the average individual molecular  $x$ ,  $y$ , or  $z$  vectors. The three alignments were achieved with two crystals. The bis(ethylenethiourea) Au(I) (AUETU2) and 3,3'-diethylthiacyanine bromide (C4) compounds belong to the triclinic crystal space group  $P\bar{1}$ . For these crystals, the two sets of molecular vectors per unit cell are related by inversion symmetry and are not constrained to lie along specific crystal axes. The individual

molecular vectors were used to define the crystal orientation vectors. For these two compounds, one crystal per orientation was required, giving a total of three crystals for AUETU2 and two crystals for C4.

The specific alignment vectors used for each of the four crystals, their angular deviations from the crystal axes, and the resulting percent molecular  $x$ ,  $y$ , and  $z$  polarizations are given in Table 4. The largest source of error in these polarized measurements is due to misalignment of the samples in the beam; however, we estimate that the maximum misalignment of the goniometer mount on the beamline is  $2^\circ$ , resulting in less than a 5% loss of polarization. After the data at the proper  $\varphi$  setting were measured, the crystal was misaligned  $2-5^\circ$  and a separate scan was measured to ensure that the spectral features noted were not due to Bragg diffraction peaks from the crystal lattice planes. Any Bragg peaks detected in this fashion were removed from the data prior to averaging by interpolation.

**Polarized Surface Measurements of Silver Bromide Sheet Crystals.** Surface X-ray measurements at glancing angle configurations take advantage of the fact that X-rays undergo total external reflection below the critical incidence angle,  $\Phi_c$ , and therefore penetrate only 20–30 Å into the surface.<sup>22</sup> At angles less than the critical angle, the signal of an

(22) Heald, S. M.; Keller, E.; Stern, E. A. *Phys. Lett.* 1984, 103a, 155–158.

Table 4. Single-Crystal Orientation Data

sample	crystal orientation vector	angular deviation from crystal axes			percent polarization <sup>a</sup>			space group	ref
		a	b	c	x <sup>b</sup>	y	z <sup>b</sup>		
M4	X	90	0	90	68	31	1	<i>P</i> 2 <sub>1</sub> / <i>c</i>	15
	Y	38.9	90	60.4	31	69	<1		
	Z	125.7	90	26.5	<1	<1	99		
DCA	X	90	90	13	74	26	0	<i>P</i> 2 <sub>1</sub> / <i>a</i>	17
	Y	90	0	90	26	74	0		
	Z	0	90	103	0	0	100		
AUETU2	X	139.8	98.8	53.5	76	24	<1	<i>P</i> $\bar{1}$	18
	Y	52.7	129.9	39.5	22	78	<1		
	Z	75.7	138.3	104.1	<1	2	98		
C4	Z-parallel	86.6	79.2	28.1	in plane		out of plane	<i>P</i> $\bar{1}$	16
	Z-perpendicular	142.6	113.0	64.3	0	100	0		

<sup>a</sup> Percent polarization based on  $\cos^2 \theta$  rule for dipole-coupled transitions, where  $\theta$  is the angle between the alignment vector and the individual molecular *x*, *y*, and *z* axes. <sup>b</sup> For C4, *x* corresponds to the in-plane orientation and *z* corresponds to the out-of-plane orientation.

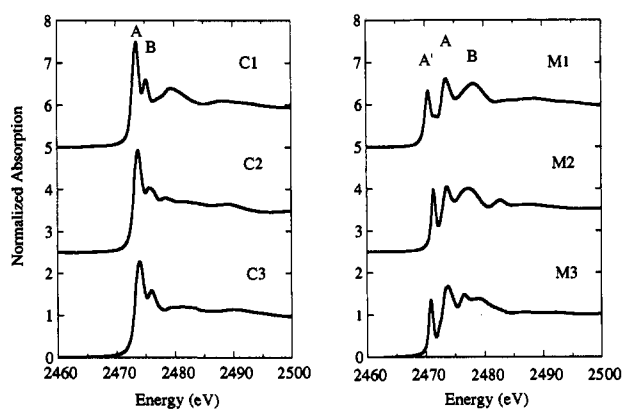


Figure 1. S K-edge spectra of representative cyanine (left) and merocyanine (right) dyes and dye nuclei (see Table 1 for abbreviations). Note the presence of a sharp feature at 2470–2472 eV (feature A') in the merocyanine dye spectra, which is not present in the spectra of the cyanine dye molecules.

adsorbed species on the surface of a substrate is enhanced relative to that of the substrate due to the decreasing penetration depth of the incident radiation. The critical angle is dependent on the type of substrate from which the X-rays reflect and is governed by the following equation for  $\Phi_c$  in radians:<sup>23</sup>

$$\Phi_c = \lambda(5.4 \times 10^{10}(Z\rho/A))^{1/2} \quad (3)$$

where  $\lambda$  is the wavelength of radiation (cm), *Z* the atomic number,  $\rho$  the density, and *A* the atomic weight of the substrate. For a AgBr substrate, the critical angle (in degrees) ranges from 1.13 at the S K-edge (2470 eV) to 1.02 at the end of a typical sulfur scan (2740 eV) and from 0.987 at the Cl K-edge (2820 eV) to 0.883 at the end of a chlorine scan (3150 eV). The measurements reported for this work were done at angles of 1°, which was sufficient at all energies to obtain an acceptable signal-to-noise level. The surface samples were mounted on a sample plate attached to a rotation stage, thereby allowing full  $\varphi$  rotations to be made (in the azimuthal plane). The sample plate and rotation stage were placed on a 90°  $\chi$  circle mounted perpendicular to the beam to allow both in-plane and out-of-plane orientations to be collected at grazing incidence angles.

## Results and Discussion

**S K-Edge Spectra of Dye Nuclei. Powder Spectra.** The unpolarized sulfur K-edge spectra for a series of cyanine and merocyanine sensitizing dye nuclei are compared in Figure 1. The energy positions of the spectral features indicated in this figure are given in Table 1. Data on additional dye compounds of this type may also be seen in the supplementary material (Figures S1 and S2 and Tables S-I, S-II, and S-III).

(23) Agarwal, B. K. In *X-ray Spectroscopy*; MacAdam, D. L., Ed.; Springer Series in Optical Sciences; Springer-Verlag: Berlin, 1979; Vol. 15, pp 130–137.

The cyanine dye nuclei contain cyclic sulfur in five-membered rings such as thiazole, benzthiazole, and naphthiazole with various ring substituents and bridges between the dye nuclei. The sulfur K-edge spectra of these heterocyclic sulfur centers are characterized by two features: a high-intensity feature at 2473.3–2474.1 eV (feature A) and a lower-intensity transition at 2475.2–2476.4 eV (feature B) observed as a high-energy shoulder on the main spectral feature, A. The relative intensities of these features and the shape of the multiple-scattering regime (above ~2478 eV) reflect changes in the local environment of the S atom. The energies of features A and B are relatively invariant; however, the features appear at a slightly higher energy for cyanine-type molecules that contain aromatic groups, such as the benzthiazole (C2, C4, C6, C7, C8, and C9) and naphthiazole (C3) derivatives (feature A at 2473.8–2474.0 eV; feature B at 2475.8–2476.4 eV) relative to the nonaromatic thiazole compounds (C5, C1: feature A at 2473.3–2473.5 eV, feature B at 2475.2–2475.3 eV). This suggests that the presence of the aromatic groups produces a more positive charge on the sulfur atom center relative to the nonaromatic-group-containing dyes and dye intermediates.

Merocyanine dyes contain sulfur as a terminal thione group on five- or six-membered heterocyclic rings such as thiohydantoin, thiobarbituric acid, and rhodanine nuclei. Like the cyanine dye nuclei, the merocyanine spectra have a prominent feature between 2473.4 and 2474.0 eV (Figure 1, feature A). This feature is less intense relative to the edge jump in the merocyanine dye spectra than in the cyanine dye spectra (Figure 1). The shoulder on the high-energy side of feature A in the cyanine dye spectra is absent in the merocyanine dye spectra; however, a broad feature that in some cases has a low-energy shoulder is seen in all of the merocyanine dye spectra (2475.4–2478.2 eV, feature B). The most striking difference between the merocyanine and cyanine dye spectra occurs to the low-energy side of feature A. The merocyanine dye spectra are characterized by a low-energy sharp bound-state feature (feature A') at 2470.5–2472.5 eV, which has no counterpart in the cyclic sulfur environment of the cyanine dye nuclei. The intensity and energy position of this feature is affected by the exact electronic and structural environment, but its presence is characteristic of all of the compounds containing the terminal sulfur moiety.

**Single-Crystal Polarized Spectra.** The intense bound-state features present in the low-energy region of the sulfur K-edge powder spectra are expected to be highly orientationally dependent for the anisotropic sulfur environments in sensitizing dye environments. Single-crystal polarized spectra were measured for both a cyanine dye, C4, and the merocyanine dye nucleus, 2-thiohydantoin (M4). The polarized measurements permit the determination of the angular dependence of and aid in the assignment of the transitions giving rise to the K-edge features observed in the powder spectra of these two classes of dye compounds.

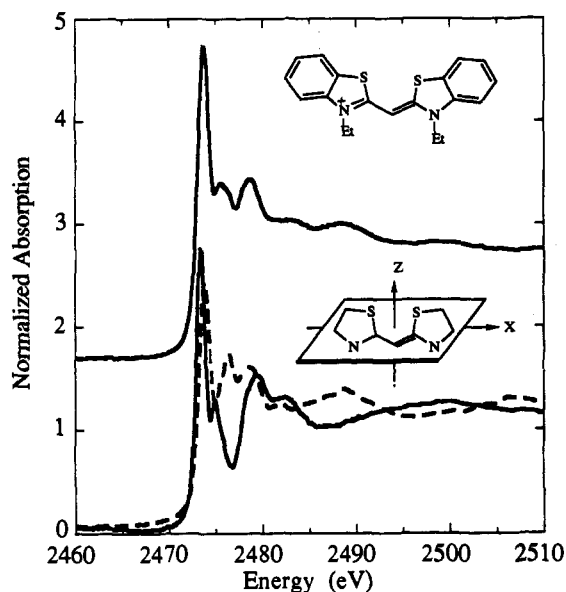


**Figure 2.** Powder spectrum (top) of C4, a cyanine dye molecule, compared with the single-crystal polarized spectra (bottom) corresponding to polarization along the *X* (solid) and *Z* (dash) molecular axes.

Single-crystal polarized spectra of the benzthiazole-containing cyanine dye molecule 3,3'-diethylthiacyanine bromide (C4) are presented in Figure 2. Spectra were obtained for two polarizations, one corresponding to polarization in the plane defined by the benzthiazole groups (C4X) and the other corresponding to polarization along the average normal to that plane (C4Z). In the powder spectrum, the most intense feature, A, occurs at 2473.8 eV, and feature B appears at 2475.6 with a shoulder at 2476.4 eV. The polarized spectra reveal contributions from both the in-plane and out-of-plane polarizations to all of the dominant spectral features observed in the powder spectra.<sup>24</sup> The appearance of these features in the powder spectra is attributed to energy splittings between the in-plane and out-of-plane polarized transitions in these spectral regions. In the in-plane polarized spectrum, the intense feature, A, occurs at 2473.5 eV, and in the out-of-plane polarized spectrum this feature is shifted to a slightly higher energy of 2473.9 eV. The feature is somewhat more intense in the in-plane polarized spectrum, but there is a strong contribution in the spectral region of feature A from bound-state transitions to final states of both  $p\sigma$  and  $p\pi$  symmetry. In the region of feature B, the in-plane polarized spectrum reveals a transition at 2475.1, while the out-of-plane polarized spectrum has more intense partially resolved split features at 2475.6 and 2476.5 eV.

Previous soft X-ray studies and calculations have been done for a variety of S heterocycles, thiols, and thioethers.<sup>12,13</sup> In these studies, the dominant feature in the S K-edge spectra occurs between 2472.3 and 2473.4 eV (relative to the  $t_{1u}$  resonance of SF<sub>6</sub> at 2486 eV), similar to the location of the strongest feature in the cyanine dye compounds. This feature has been assigned to a transition to a S-C final state with  $\sigma^*$  symmetry,<sup>10,12,13</sup> which supports the qualitative determination of the symmetry of this feature based on our polarized single-crystal study. In a study of the aromatic molecule thiophene,<sup>12a</sup> multiple scattered wave X $\alpha$  calculations showed that the lowest unoccupied valence orbital has  $\pi^*$  symmetry and occurs at approximately the same energy as the S-C  $\sigma^*$  orbital. The aromatic character of thiophene allows appreciable delocalization of the  $\pi^*$  level onto the sulfur atom, accounting for approximately 25% of the intensity of the 2473 eV feature, with the balance being accounted for by the transition to the S-C  $\sigma^*$  orbital. It is therefore likely that the *z*-polarized contribution to the 2474 eV region absorption feature results

(24) For in-plane polarized spectra, transitions occur to orbitals of  $p\sigma$  symmetry, while transitions to orbitals of  $p\pi$  symmetry occur for out-of-plane polarized spectra.

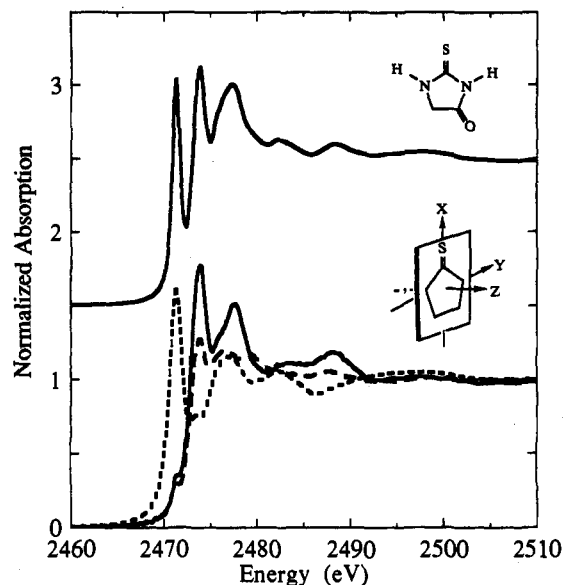


**Figure 3.** Powder spectrum (top) of M4, a merocyanine dye nucleus, compared with the single-crystal polarized spectra (bottom) corresponding to polarization along the average *X* (solid), *Y* (dash), and *Z* (dot) molecular axes. The *Z* orientation is 99% polarized along the molecular *z* axis. The *X* and *Y* orientations are 68–69% polarized, containing approximately 31% of the other in-plane polarization. Note that the intense low-energy feature at ~2471 eV is *z*-polarized and the primary absorption feature at ~2474 eV is *x*-polarized.

from a transition to a final state with  $p\pi$  symmetry due to the extended conjugated system of 3,3'-diethylthiacyanine bromide.

The single-crystal polarized spectra for 2-thiohydantoin (M4), a merocyanine dye nucleus, are presented in Figure 3. Three orientations were isolated: two in-plane orientations maximizing polarization either parallel or perpendicular to the C=S bond (*X* or *Y* polarization, respectively) in the plane of the thiohydantoin ring and an out-of-plane orientation perpendicular to the ring (*Z* polarization). The crystallographic constraints of the molecule result in the *Z* orientation being nearly 100% polarized, while the *X* and *Y* orientations are each approximately 69% polarized, containing 31% polarization of the other in-plane polarization. Unlike the cyanine dye, the polarized spectra of 2-thiohydantoin reveal that the features observed in the powder spectrum are strongly polarization dependent. The sharp pre-edge feature A' at 2471.2 eV, characteristic of the terminal thione sulfur, is polarized almost entirely along the normal to the plane of the 2-thiohydantoin molecule and is assigned as a transition to a final state of  $p\pi$  symmetry due to the presence of unfilled C=S  $\pi^*$  orbitals for molecules of this type. In contrast, the intense feature A at 2473.7 eV is polarized in the plane of the molecule, predominantly along the C=S bond, and is assigned as a transition to a final state of C-S  $\sigma^*$  symmetry.

There are striking differences in the spectra of molecules containing sulfur in an exocyclic (thione) environment compared to that of the cyclic sulfur (thiazole) environment. The intense feature A occurs at about the same position for all of the compounds studied, but is more intense for the thiazole compounds than for those containing thione. This feature is polarized along the C-S bond in the thione compound and corresponds primarily to a transition to the C-S  $p\sigma^*$  orbital. In the cyclic sulfur compounds, a transition to a  $p\pi$  orbital also contributes to the intensity of this feature. For the exocyclic S compounds, only a transition to the C-S  $p\sigma^*$  orbital contributes to this feature. This difference could account for the increase in intensity of this spectral feature for thiazoles relative to thiones. In addition, the low-energy feature A' is seen for compounds in which S is present as a thione and is absent in the cyclic sulfur compounds. The presence of this feature is due to a transition to a final-state  $p$  orbital arising from the involvement of the exocyclic sulfur in a

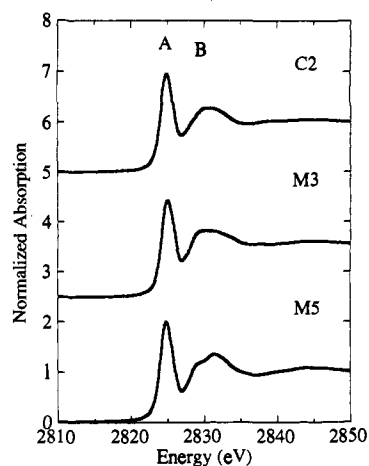


Figure 4. Cl K-edge spectra of representative dyes and dye nuclei (see Table 1 for abbreviations).

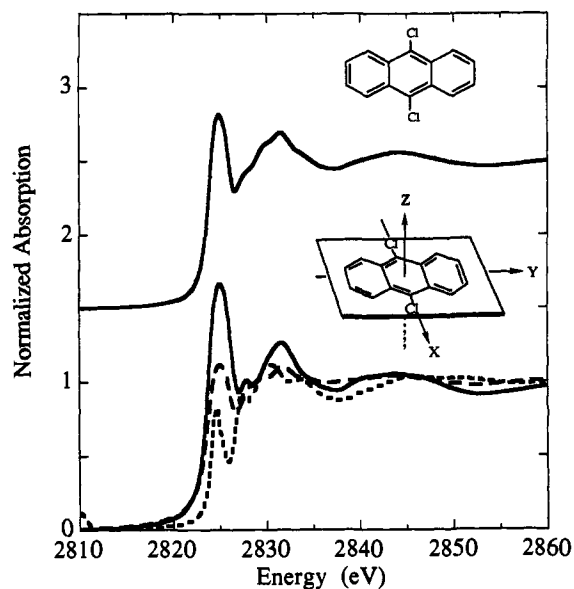


Figure 5. Cl K-edge powder spectrum (top) of DCA, compared with the single-crystal polarized spectra (bottom) corresponding to polarization along the average  $X$  (solid),  $Y$  (dash), and  $Z$  (dot) molecular axes. The  $Z$  orientation is 100% polarized. The  $X$  and  $Y$  orientations are 74% polarized, containing 26% of the other in-plane polarization.

$p\pi$  system and was found to be polarized perpendicular to the C=S bond and the plane of the ring.

**Cl K-Edge Spectra of Dye Nuclei.** Investigation of the X-ray absorption properties of the Cl centers present as substituents in dyes can provide another probe of the electronic and structural environment of these molecules. Cl K-edge spectra were measured for a series of Cl-substituted dyes (Figure 4 and Table 1). The observed spectral features were found to be very similar in all of the compounds studied, revealing a single high-intensity feature between 2824.8 and 2825.1 eV and a broad higher-energy feature occurring between 2829.1 and 2830.6 eV, characteristic of the C-Cl environment present in all of these compounds. The intensity and energy position of the prominent absorption feature appears to be relatively insensitive to structural changes in the dye systems more remote from the Cl centers, but a strong polarization dependence of the Cl K-edge spectra is observed.

To understand the polarization properties of Cl as a substituent on dye molecules, single-crystal polarized studies on  $\beta$ -9,10-dichloroanthracene (DCA) were performed. The powder spectrum of DCA has the same spectral features as the Cl K-edge spectra of the dye samples, making it an appropriate choice for the single-crystal studies. The polarized single-crystal and powder spectra of DCA are compared in Figure 5. The three single-crystal spectra correspond to polarizations in the plane of the

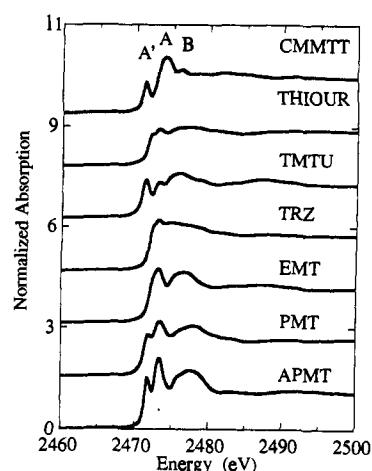


Figure 6. S K-edge spectra of terminal sulfur thione- and thiol-containing ligands (see Table 2 for abbreviations).

molecule, maximizing polarization either parallel or perpendicular to the Cl-Cl vector ( $X$  and  $Y$  polarization, respectively) or perpendicular to the plane of the molecule ( $Z$  polarization). The crystallographic constraints of the DCA molecule result in the  $Z$  orientation, reflecting nearly complete  $z$  polarization, while the  $X$  and  $Y$  orientations are only approximately 74% polarized along their respective molecular axes, each containing 26% of the other in-plane polarization direction.

A comparison of the powder and oriented single-crystal spectra reveals that the dominant spectral features observed in the unpolarized spectrum contain contributions from all three molecular polarizations. The  $X$  orientation, however, shows the highest intensity in the region of the intense feature at 2825.0 eV. A less intense contribution in this spectral region is also observed in the  $Y$  orientation due primarily to the incomplete polarization obtained with this crystal. In the  $Z$ -polarized spectrum, a feature is also observed in this spectral region that is shifted to a slightly lower energy of 2824.6 eV and is a much narrower transition than the corresponding in-plane-oriented spectra, indicating that there may be multiple transitions occurring in the in-plane orientation. These results suggest that the intense K-edge feature of compounds containing Cl in this kind of an environment is primarily due to a transition to a final-state orbital with  $\sigma$  symmetry with some contribution from a near-lying lower-energy  $p\pi$  orbital. Similarly to what has been reported for thiophene,<sup>12a</sup> the presence of the low-energy feature in the out-of-plane polarized spectrum indicates the involvement of the Cl  $p\pi$  orbitals in the aromatic  $\pi$  system of DCA. The complicated shape of the spectral region to the high-energy side of the main absorption peak is due to the many overlying transitions resulting from both in-plane and out-of-plane polarized transitions. This higher-energy region probably reflects transitions to less localized final-state orbitals that are sensitive to the very anisotropic intra- and intermolecular scattering interactions of the Cl centers in this molecule.

Cl K-edge spectra have been reported for  $\text{SCl}_2$ ,  $\text{S}_2\text{Cl}_2$ ,  $\text{SOCl}_2$ , and  $\text{SO}_2\text{Cl}_2$ .<sup>12d,e</sup> For these compounds, the Cl K-edge spectra are similar to those of the organic dye molecules studied here, with the most intense feature occurring between 2821.4 and 2822.5 eV. This feature has been assigned as a transition to a final state with S-Cl  $\sigma^*$  symmetry, supporting the qualitative conclusion that the predominant feature in the Cl K-edge of the dye molecules can be attributed to a transition to a final state with C-Cl  $\sigma$  symmetry.

**Sulfur K-Edges of Surface-Modifying Ligands.** In addition to the merocyanine dye nuclei discussed above, sulfur K-edge absorption data were collected on powder samples of a variety of other terminal sulfur compounds including thioureas, mercaptotetrazoles, thiazoline thione, and triazolium thiolate (Table 2). The powder spectra of these compounds are compared in Figure 6. All of these compounds may act as silver ligands in



photographic materials. The structures indicated in Table 2 represent the thioureas and the thiazoline thione compounds in their thione form, the mercaptotetrazoles are represented as thiols, and the triazolium thiolate as a thiolate structure. For all of these compounds, however, there are other resonance and tautomeric forms possible in which the sulfur centers may be represented as alternate thione/thiol(ate) structures with varying degrees of C–S double-bond character and negative charge on the sulfur center. The TRZ compound is a mesoionic molecule that cannot be represented as a single resonance form without invoking formal atomic charges. It may be represented as either a thione or thiolate form. In Table 2, it has been represented in its thiolate form, with a negative charge on the terminal S and a delocalized positive charge in the ring system.

Similarly to what was observed with the merocyanine dye nuclei, the K-edge spectra of these compounds exhibit the low-energy A and A' features. The relative intensities and energy positions of these features are strongly influenced by the exact structural and electronic environment of the sulfur centers in the ligand compounds. The lower-energy feature, A', which has been assigned to a  $1s \rightarrow p\pi^*$  transition on the basis of the polarized measurements of 2-thiohydantoin, is present in all of the spectra; however, its energy position and resolution from feature A is strongly sample dependent.

The compound 3-(carboxymethyl)-4-methyl-4-thiazoline-2-thione (CMMTT) contains both heterocyclic and exocyclic sulfur centers. The spectrum of this compound reflects a superposition of the features characteristic of both the thione and thiazole S, with the well-resolved A' feature at 2471.4 eV due to the thione S and the broader high-intensity feature A at 2474.3 eV containing intensity contributions from transitions involving both the terminal and cyclic sulfur. The spectra of the two thiourea compounds differ significantly in the energy position and intensity of the A' feature. In the case of the tetramethyl thiourea, the A' feature is observed as a well-resolved feature at 2471.4 eV, while in the unsubstituted thiourea, this feature is observed as a lower-intensity, partially resolved feature at a higher energy position of 2472.0 eV. The A' feature is also reduced in intensity and observed at a higher energy for the mesoionic TRZ compound. Three different mercaptotetrazole compounds were investigated, and the energy position and intensity of the A' feature are a function of the  $\alpha$ -N substituent in this compound. For the ethyl-substituted compound (EMT), the A' feature at 2472.5 eV is low in intensity and poorly resolved from the prominent spectral feature, A, while for the phenyl-substituted compounds, PMT and APMT, the A' feature is more clearly resolved and lower in energy (2471.8 eV).

The intensity and energy position of the low-energy  $1s \rightarrow p\pi^*$  transition corresponding to the A' feature are, thus, a sensitive probe of the electronic environment of terminal sulfur groups. Tautomeric and resonance forms that reduce the double-bond character of the C–S bond result in a shift to higher energy and an intensity reduction of this spectral feature. This is observed in the case of the thiourea and mercaptotetrazole compounds, where hydrogen bonding between the terminal SH group and the  $\alpha$ -N atoms will influence the double-bond character of the C–S bond as a function of the nature of the substituent on the other  $\alpha$ -N. Similar observations in the sensitivity of S, N, and O K-edge spectral features have been used to investigate keto-enol(ate) tautomeric resonance of other amides and thioamide compounds.<sup>25</sup> The phenyl-substituted mercaptotetrazole compounds, PMT and APMT, extend the  $\pi$  system of the molecule. The  $\pi$  character of the C–S bond in these compounds (as evidenced by a more well-resolved A' feature) is greater than that of the ethyl-substituted analog, EMT. The low intensity and higher energy position of the A' feature for the TRZ compound would

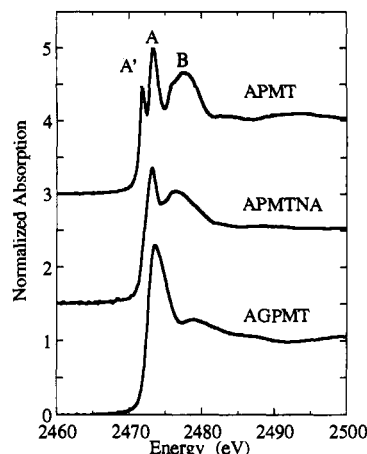


**Figure 7.** Powder spectra of different mercaptotetrazole forms: (top) protonated free-acid form (APMT); (middle) sodium salt of the deprotonated thiolate form (APMTNA); (bottom) a 1:1 silver complex of a related deprotonated mercaptotetrazole ligand (AGPMT). Both deprotonated forms result in the disappearance of the low-energy feature (A'). An increase in the intensity of the dominant feature (A) is observed for the covalent complex with silver but not for the ionic sodium salt.

be consistent with the thiolate form of this compound being its predominant resonance form. In this resonance form, the terminal sulfur has little C–S double-bond character and carries a significant negative charge on the sulfur atom.

MOPAC<sup>26</sup> calculations of the ground-state orbitals of terminal sulfur ligands such as 2-thiohydantoin and thiourea revealed the presence of two low-lying unoccupied orbitals of  $\pi$  and  $\sigma$  symmetry. For these thione ligand forms, the  $\pi$  LUMO, which contained  $\sim 20$ – $25\%$  contribution from the S  $p_x$  orbital, was calculated to be 1.0–1.5 eV lower in energy than the  $\sigma$  (LUMO +1) orbital, which contained  $\sim 40$ – $45\%$  contribution from the S  $p_x$  orbital. In contrast, calculations of protonated thiol(ate) tautomeric or resonance forms of these types of ligands resulted in a decrease in the energy splitting between the two lowest-lying unoccupied molecular orbitals and a significant reduction or complete loss of the S  $p_x$  character of the LUMO.

There have been some S K-edge studies of compounds containing a terminal sulfur group reported.<sup>12b,c,13</sup> In these studies, both CS<sub>2</sub> and SCO have features below 2473 eV (at 2470.8 for CS<sub>2</sub> and 2472.0 for SCO), which have been assigned to transitions with final states of  $\pi$  symmetry, consistent with the qualitative results of the polarized single-crystal measurements on 2-thiohydantoin reported herein. In contrast to the mercaptotetrazoles studied here, there is no low-energy pre-edge feature seen in the S K-edge spectra of the alkyl thiols studied by Dezarnaud et al.<sup>12b</sup> The primary difference between the alkyl thiols and the mercaptotetrazoles in this work is the presence of the conjugated  $\pi$  system in the mercaptotetrazoles. This difference is consistent with the presence of the low-energy feature reflecting involvement of the terminal S group in the  $\pi$  system, whether it be through a formal C=S double bond or the presence of a conjugated  $\pi$  system.

In Figure 7, the spectra of two different forms of the APMT compound are compared with that of a silver complex of the PMT ligand. The protonated free-acid form of APMT reveals the well-resolved A' feature at 2471.8 eV, indicating a high degree of C–S double-bond character. In contrast, the deprotonated sodium salt, APMTNA, has only a very weak shoulder in the A' spectral region at 2472.2 eV, reflecting the nearly fully occupied  $p\pi$  orbital in the negatively charged form of the mercapto compound. The appearance of the primary absorption feature, A, due to a transition to a  $p\sigma$  final-state orbital, is very similar for the protonated and deprotonated forms of this compound, indicating that the C–S  $\sigma$  bond is not influenced significantly by

(25) (a) Oichi, K.; Ito, H.; Seki, K.; Araki, T.; Narioka, S.; Ishii, H.; Okajima, T.; Yokoyama, T.; Ohta, T.; Inabe, T.; Maruyama, Y. *Jpn. J. Appl. Phys.* 1993, 32-2 (Suppl.), 818–820. (b) Araki, T.; Seki, K.; Narioka, S.; Ishii, H.; Takata, Y.; Yokoyama, T.; Ohta, T.; Okajima, T.; Watanabe, S.; Tani, T. *Jpn. J. Appl. Phys.* 1993, 32-2 (Suppl.), 815–817.

(26) Dewar, M. J. S. *J. Mol. Struct.* 1983, 100, 41–50.

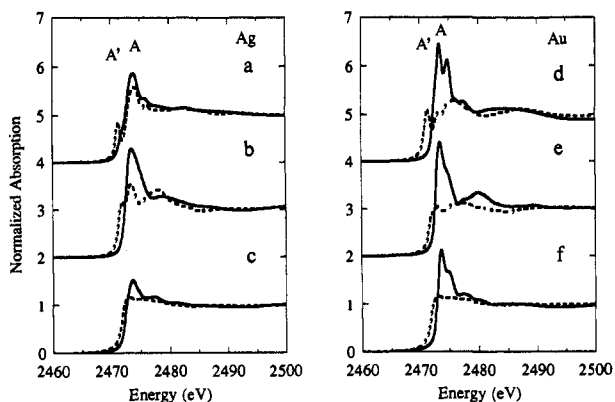


**Figure 8.** Powder spectra of Ag and Au complexes (solid) compared to the spectra of the uncomplexed terminal sulfur ligands (dot) described in Tables 2 and 3: (a) AGCMMT and CMMT; (b) AGPMT and PMT; (c) AGTRZ2 and TRZ; (d) AUTMTU and TMTU; (e) AUTHIO and THIOUR; (f) AURZ2 and TRZ. Note the absence of the low-energy feature (A') and the increase in intensity of the dominant spectral feature (A) in the metal complexes relative to the ligand spectra. The increase in the intensity of feature A is greater with Au complexation than Ag.

the deprotonation or interaction with the sodium counterion. In comparison to the sodium salt, the silver complex of the deprotonated PMT compound reveals a primary absorption feature, A, which is significantly enhanced in intensity relative to that of the uncomplexed PMT ligand spectrum. This spectral change is evidence of a direct bonding interaction between the negative sulfur center and the silver metal ion, which is not present in the sodium salt.

**Au and Ag Complexes of Terminal Sulfur Ligands. Powder Spectra.** SK-edge XAS spectra were measured for a wide variety of complexes formed between Ag or Au and terminal sulfur ligands including 3-(carboxymethyl)-4-methyl-4-thiazoline-2-thione, thioureas, phenylmercaptotetrazole, and triazolium thiolate (Table 3). These compounds were chosen to investigate the effect that Ag or Au metal complexation would have on the electronic structure of sulfur ligands representative of photographic surface species. A comparison of representative ligand and metal-ligand complexes is presented in Figure 8. In all of the metal-sulfur compounds, the intense primary absorption feature, A, increases in intensity and the low-energy A' feature between 2470.5 and 2472.0 eV is absent. The absence of the low-energy transition to the ligand  $\pi\pi^*$  orbital in these metal complexes suggests that the  $\pi\pi^*$  orbital of S is directly involved in the covalent metal-sulfur interaction.

The presence of gold has a much stronger effect on the SK-edge spectra than silver. In general, the intensity of the primary absorption feature, A, of the Au complexes studied here, is greater than that of the Ag complexes. This feature in the Au complexes is also more narrow than in the Ag complexes, indicating a more localized final-state orbital in the Au-S complexes. In addition, a shoulder can be seen on the high-energy side of the main Au-S transition that is sometimes well-resolved. In the Ag complexes, the main transition is broadened to the high-energy side; however, no shoulder is resolved from this feature.

**Single-Crystal Polarized Studies of a Au-S Complex.** Single-crystal polarized sulfur K-edge spectra were measured on bis-(ethylenethiourea) Au(I) hydrate hydrochloride (AUETU2), in which the Au metal forms a nearly linear two-coordinate complex with the terminal S ligand (Table 2). The powder spectra of AUETU2 and the uncoordinated ethylenethiourea (ETU) ligand are compared to the polarized spectra of the AUETU2 single crystals in Figure 9. For the polarized measurements, X was defined to be in the plane of the ligand rings along the average C-S<sub>thione</sub> bond, Z was defined to be the average of the ligand plane normals, and Y, defined to be the cross product of X and Z, is directed roughly along the S-Au-S bond. The individual

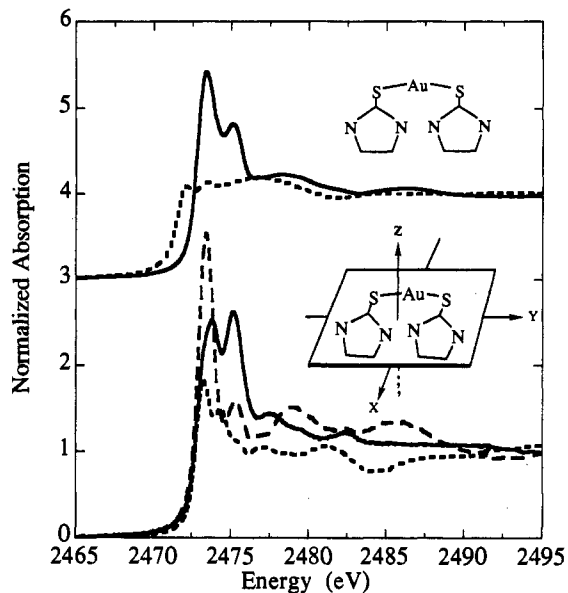


**Figure 9.** Powder spectrum of AUETU2 (solid) compared to the spectrum of the ETU ligand (dot) (top) and the single-crystal polarized spectra of AUETU2 compared for polarizations along the average X (solid), Y (dash), and Z (dot) molecular axes (bottom). The Z orientation is 98% z-polarized. The X and Y orientations are 76-78% polarized along the individual ligand x and y axes, each containing 22-24% of the other in-plane polarization.

ETU ligand planes are not completely coplanar, with a dihedral angle of approximately  $12^\circ$ . The individual ligand x and y axes, defined analogously to those used in the single-crystal orientations of the thiohydantoin molecule (M4), deviate from the average molecular alignment vectors, X and Y, by approximately  $29^\circ$ . As a result, the defined crystal orientation vectors result in ligand polarizations that are 98% for Z and 76% and 78% for alignment along X and Y, respectively.

The direct interaction of the ligands with the Au ion in this complex has a pronounced effect on the sulfur K-edge features. In the powder spectrum of AUETU2, the partially resolved low-energy feature, A', at 2472.0 eV in the uncomplexed ligand is absent, and the primary feature, A, is significantly enhanced in intensity. In addition, the gold complex spectrum contains a second intense higher-energy feature at 2475.3 eV. The polarized spectra reveal that the features in the powder spectrum of AUETU2 are polarized primarily in the plane of the ligand rings. The most intense polarized feature is observed in the Y-polarized spectrum. This feature occurs in the same energy region as the feature A in the powder spectrum at 2473.4 eV. The X-polarized spectrum reveals two intense spectral features at 2473.9 and 2475.3 eV. Since both of these features are X-polarized, they must result from transitions to final states involving the S  $p_x$  orbitals. The presence of two features suggests that a direct Au-S  $\pi$  interaction produces two final states of  $p_x$  symmetry with an energy splitting of 1.4 eV. In contrast, a single intense transition of S  $1s \rightarrow C-S \sigma^*$  symmetry was observed in the X-polarized spectrum of the uncomplexed M4 ligand (see Figure 3). The feature at 2475.3 eV in the AUETU2 powder spectrum has no counterpart of comparable intensity in the pure ligand spectrum. Its dominance in the X-polarized spectrum of the metal complex indicates that it is due to a transition to a final state involving the sulfur  $p_x$  orbitals in a metal-S  $\pi$  interaction.

In the Z-polarized spectrum of the AUETU2 complex, there is a feature observed at 2473.2 eV. In comparison, no transition in this energy region is observed for the out-of-plane polarization of the uncomplexed terminal sulfur ligand, 2-thiohydantoin (see Figure 3). For the uncomplexed ligand, the Z-polarized A' feature is observed 1.2 eV lower in energy at 2472.0 eV. The presence of the 2473.2 eV feature in the out-of-plane spectrum of AUETU2 must, therefore, be due to a metal-sulfur  $\pi_z$  interaction and

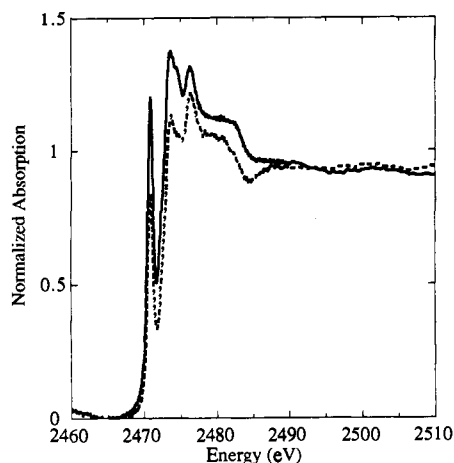


**Figure 10.** S K-edge surface spectra of a AgBr sheet crystal treated with merocyanine dye M3 measured at  $\chi = 0^\circ$  (solid) and  $\chi = 90^\circ$  (dash).

indicates a shift in the energy of the ligand C=S  $\pi^*$  orbital as a result of admixture between the ligand and metal orbitals.

Extending these results to the powder spectra of the other metal-sulfur complexes, it may be concluded that the intense feature at 2473 eV is due to two transitions to final states of S  $\sigma$  interactions: one resulting from a dominant interaction involving S  $p_y$  orbitals with metal-S  $\sigma$  character and the other involving the S  $p_x$  orbitals with C-S  $\sigma$  character and Au-S  $\pi_x$  character. This latter feature is shifted to a higher energy than that of the C-S  $\sigma$  feature in the uncomplexed terminal sulfur ligands as a result of the influence of the  $\pi$  interaction between the metal and ligand orbital. The appearance of a shoulder or partially resolved feature at 2475 eV on the high-energy side of the dominant spectral feature is further evidence of a direct metal-S  $\pi$  interaction involving S  $p_x$  orbitals. In Figure 7 the spectra of mercaptotetrazole ligands were compared for the free-acid, sodium salt, and silver complex forms. In contrast to the dramatic change seen in the S K-edge spectra as a result of a covalent interaction between Ag or Au and S, an ionic interaction between S and the sodium ion results in the loss of the pre-edge peak reflecting the negatively charged terminal sulfur group but no change in the shape or intensity of the dominant absorption feature at 2473.2 eV. This suggests that, unlike the covalent metal-S interaction in the Ag complex, the ionic interaction between  $\text{Na}^+$  and S has little or no effect on the  $\sigma$ -symmetry final-state orbitals.

**Preliminary Application to Surface Measurements.** X-ray absorption data were collected at glancing incidence angle on a AgBr sheet crystal sample treated with a merocyanine dye (M3). This dye contains both S and Cl centers, thereby allowing polarized measurements at both K-edges to be used to investigate the orientation and interaction of the dye molecule with the silver bromide surface. Polarized measurements were collected corresponding to in-plane ( $\chi = 0^\circ$ ) and out-of-plane ( $\chi = 90^\circ$ ) orientations of the sheet crystal surface.

The polarized surface spectra at the sulfur and chlorine K-edges are shown in Figures 10 and 11, respectively. The thione sulfur pre-edge feature, A', observed at 2470.9 eV in the dye powder spectrum (Figure 1) is present in both the in-plane and out-of-plane orientations of the dyed sheet crystal sample (Figure 10). In addition, the prominent feature, A, at 2474.0 eV, is not increased in intensity relative to the pure dye spectrum. Both of these spectral results indicate that there is no significant covalent bond formed between the thione S and the Ag in the AgBr sheet crystal.

The sulfur K-edge features in the dyed sheet crystal do show some orientational dependence with both the A' and A features being more intense for the in-plane polarization than in the out-of-plane orientation. For the polarized K-edge measurements, intensity enhancement occurs when the polarization vector of the incident radiation is codirectional with the molecular  $x$ ,  $y$ , or  $z$  axis of interest. As discussed earlier, we have found that the

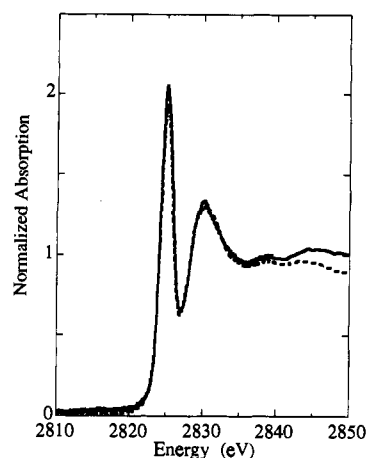


**Figure 11.** Cl K-edge surface spectra of a AgBr sheet crystal treated with merocyanine dye M3 measured at  $\chi = 0^\circ$  (solid) and  $\chi = 90^\circ$  (dash).

sulfur pre-edge feature, A', is due to a transition to a S  $p\pi^*$  orbital oriented out of the plane of the molecule, while the higher-energy feature, A, was found to be polarized along the C-S bond direction. For the intensity of both of these spectral features to increase with in-plane polarization of the sheet crystal sample, the dye molecules must be oriented on the surface such that both the dye molecule plane normals and the C-S bond directions lie in the plane of the sheet crystal surface. Such an orientation would correspond to an edge-on (or perpendicular) alignment of the dye molecules on the silver halide surface. The pre-edge A' feature does not vanish in the out-of-plane orientation, but it is about half as intense as in the in-plane spectrum. This suggests that the dye molecules are tilted with respect to the plane of the surface, resulting in some excitation into this orbital for out-of-plane polarizations.

Additional confirmation of this interpretation is indicated by the lack of any significant orientational dependence of the Cl K-edge primary absorption feature at 2825.1 eV (Figure 11). This spectral feature was found from the single-crystal polarized measurements to be predominantly polarized along the C-Cl bond direction and assigned to a Cl  $1s \rightarrow \text{C-Cl } \sigma^*$  transition. The C-Cl molecular vector would only have significant projections along the radiation polarization direction for both in-plane and out-of-plane polarizations for dye molecules oriented edge-on to the surface of the sheet crystal. If the dye molecular planes were oriented flat on (or parallel to) the sheet crystal surface, there should be very little intensity in the Cl  $1s \rightarrow p\sigma^*$  transition for the out-of-plane orientation.

The dyed AgBr sheet crystal sample did not show the dramatic change in the S K-edge features associated with a direct covalent bonding interaction between the metal and the sulfur as was observed with the other metal-sulfur complexes shown in Figure 8. This suggests either that the nature of the interaction in the dyed sheet crystal sample is of a physical, rather than a chemical, nature or that any direct bonding interaction that does occur between the dye molecules and the AgBr substrate does not involve the S atoms. Although we believe that there was only a monolayer of dye on the surface in these preliminary measurements, the possibility that we were sampling a multilayer region of the substrate and not only the substrate/adsorbate interface cannot be eliminated at this point.

## Conclusions

These studies have shown that S and Cl K-edge X-ray absorption spectroscopy is a sensitive probe of the electronic and bonding environment of sensitizing dye and silver ligand centers of significance in photographic materials. Single-crystal polarized studies have permitted the symmetry assignments of many of the spectral features observed. XAS can distinguish between covalent

and ionic interactions between a metal and exocyclic sulfur. The distinctive changes observed in the S K-edge spectra of Ag and Au metal complexes permit predictions of the nature of the dye adsorbate/AgBr substrate interaction to be made and clearly show that there is no covalent interaction between the Ag ions in the AgBr sheet crystals and the terminal S centers in the merocyanine dye molecule investigated here. In addition, the sensitivity of XAS to the polarization properties of the S K-edge features provides insight into the orientation of the dye molecules on the AgBr substrate, indicating that the dye molecules are adsorbed in an edge-on fashion.

**Acknowledgment.** This work was supported in part by research funds from Eastman Kodak Co. These data were collected at the Stanford Synchrotron Radiation Laboratory (SSRL) and at the National Synchrotron Light Source (NSLS), Brookhaven National Laboratory, which are supported by the Department of Energy, Division of Materials Sciences, and Division of Chemical

Sciences. SSRL is also supported by the National Institutes of Health, Biomedical Research Technology Program, National Center for Research Resources, and by the Department of Energy, Office of Health and Environmental Research. Funds for an upgrade of the diffractometer used in alignments were provided in part by the NSF, Grant CHE-8717071.

**Supplementary Material Available:** Table S-I and Figure S1, containing S K-edge information about the cyanine dye samples investigated, Table S-II and Figure S2, containing S K-edge information about the merocyanine dye samples investigated, and Table S-III and Figure S3, containing Cl K-edge information about the dye samples investigated (8 pages). This material is contained in many libraries on microfiche, immediately follows this article in the microfilm version of the journal, and can be ordered from the ACS; see any current masthead page for ordering information.